

Influence of twin planes in $\text{YBa}_2\text{Cu}_3\text{O}_7$ on magnetic flux movement and current flow

Rinke J. Wijngaarden and R. Griessen

Department of Physics and Astronomy, Vrije Universiteit, De Boelelaan 1081, 1081 HV Amsterdam, The Netherlands

J. Fendrich and W.-K. Kwok

Argonne National Laboratory, Argonne, Illinois 60439

(Received 1 July 1996)

The effect of twin planes in $\text{YBa}_2\text{Cu}_3\text{O}_7$ on the superconducting current flow is investigated. A single crystal containing only two twin planes is studied magneto-optically up to 1 T. It is found that flux enters the crystal very easily along the twin planes, but that it does not leave the sample preferentially along the twin planes. The flux present in the twin planes reduces the flux penetration in adjacent regions of the sample. During flux penetration, the current density across the twin plane is about half of the current density in the rest of the sample. Due to this, the shielding current breaks up into several subloops. From a simulation follows that in a thin sample flux penetration is enhanced at inward pointing irregularities of the edge of the sample. [S0163-1829(97)07805-3]

I. INTRODUCTION

Twin planes form easily during the growth process of $\text{YBa}_2\text{Cu}_3\text{O}_7$ due to the fact that the unit cell is only slightly orthorhombic. In as-grown crystals the number of twins is 5–60 twins per mm. Impurities tend to accumulate in the twin planes during growth and the typical width is of the order of a few nm. Flux movement in a superconductor leads to dissipation which is detrimental for most applications. Therefore the influence of twin planes on flux motion is of prime importance from a practical point of view. The study of the present sample also leads to some conclusions on the influence of defects on flux penetration in general.

The influence on the flux pinning properties of twin planes in $\text{YBa}_2\text{Cu}_3\text{O}_7$ has been the subject of many studies.^{1–11} The first evidence that twin boundaries are an important anisotropic pinning defect was given by Kwok *et al.*¹ The effect of the twin boundaries on the magnetization as a function of angle between twin planes and applied field was studied by Gyorgy *et al.*² and more recently by Oussena *et al.*^{3,4}

Surprisingly, some of the previous magneto-optical work reaches seemingly contradictory conclusions. In a sample with many parallel twins, Duran *et al.*⁵ observed that flux penetrated quickly along the twins. By contrast, in a similar experiment, Vlasko-Vlasov *et al.*⁶ argue that flux cannot move easily along the twins, but that these guide the flux which penetrates elsewhere because the flux cannot cross the twins. The movement of flux along and across twin planes was investigated in a carefully prepared sample by Welp *et al.*,⁷ who find that the flux moves easily along twins, while movement across the twins is strongly hindered. Also Turchinskaya *et al.*⁸ find a strong anisotropy for flux motion along and across twins, while a similar observation for thin films is made by Safar *et al.*⁹ It now seems well established^{10,11} that flux can move easily along twins but not across twins. The cross over from one behavior to the other as a function of the angle of flux movement with respect to the twin plane and as a function of relative strength of bulk

and twin-boundary pinning has been investigated by Groth *et al.*¹² by simulations.

Dorosinskii *et al.*^{13,14} report strong pinning as a bulk property of heavily twinned regions, in particular at temperatures around 60 K. Strong pinning due to twins seems to be at variance with fast flux penetration along twins because in a heavily twinned crystal there is a network of twin planes along which the flux might move easily like traffic in the streets of a town. In this work we reconcile these seemingly conflicting observations.

The main part of this paper is concerned with the detailed current flow pattern at a twin plane. This is determined using a newly developed scheme which finds the current flow in flat superconductors from magneto-optical measurements of the perpendicular component of the local magnetic field. No simplifying assumptions or *a priori* knowledge about the flow pattern is necessary.

After a description of the high-field, high-resolution magneto-optical experimental technique, we show some simulations on the effect of defects on the current flow and magnetic field, which show that the flux penetration at the twin planes, which is higher due to reduced pinning, is further enhanced by an increased local magnetic field. Then experimental results for flux flow along and across twin planes in a crystal with two twin planes only will be presented as well as for the asymmetry between flux entering and leaving the sample. In a subsequent section the current flow pattern is given and the effect of the twins on the flow pattern is discussed. Finally conclusions are drawn.

II. EXPERIMENT

$\text{YBa}_2\text{Cu}_3\text{O}_7$ crystals were grown in a gold crucible by a self-flux method. The crystals were individually detwinned by the application of uniaxial stress. One crystal was selected in which precisely two twin planes remained. Its dimensions are $700 \times 400 \times 25 \mu\text{m}^3$.

For the magneto-optical experiments we used EuSe as an indicator of the local magnetic field, which enables studies

up to fields of 1 T. A glass substrate was first covered by 250 nm EuSe and then by a reflecting 100 nm aluminium layer. The YBa₂Cu₃O₇ crystal was mounted on the glass plate in direct contact with the aluminum. This assembly was mounted in our homebuilt cryogenic polarization microscope,¹⁵ which is in the variable temperature insert of an Oxford Instruments 1 T magnet system. The c axis of the sample is perpendicular to the aluminum and EuSe layers and parallel to the externally applied field. Polarized light propagating parallel to this c axis passes through the EuSe layer, is reflected by the aluminum layer, and passes again through the EuSe. Due to the large Faraday effect of EuSe at temperatures below 10 K, the spatial variation of the perpendicular component of the local magnetic field H_z is made visible after the analyzer of the microscope as an intensity pattern. Using a low light level CCD camera (Tokyo Electronic Industry CS8320C) this pattern is recorded by a video cassette recorder (Sony EVO-9650P) with time code. The time code is a number attributed to each individual video image; it is stored together with the experimental conditions such as temperature and applied field in a computer file. Images are grabbed and digitized using a Videopix framegrabber in a SUN workstation.

To correct for possible uneven illumination a so-called illumination image is taken with uncrossed polarizers in zero applied field and above T_c . After subtraction of an offset (due to the electronics) of both images, any raw magneto-optical image is divided by the illumination image. The local field H_z is found using the calibration $I = \beta f(H_z^2)$, where I is the intensity and β is a proportionality constant. The function f is determined in a separate (calibration) experiment, while β can be found if the field is *a priori* known at a certain position in the image. Since far away from the sample the local field is equal to the known applied external field,

this is no problem. During one experimental run β is, in principle, constant thus this inversion can also be used close to zero field, where direct calibration of β would not be very accurate because both I and f are very small. In this way the field H_z may be determined except for its sign, because of the quadratic dependence in f . The sign is generally known from the history of the experiment, but may be determined experimentally by turning the analyzer.

III. LOCAL MAGNETIC FIELD AROUND DEFECTS: A SIMULATION

Before discussing our experiments it is illustrative to show the results of a few simulations, where we calculate the local field in a sample containing defects. If an external field is applied to a superconductor, currents are induced which shield the inside from the external field. The field produced by the shielding current is called the self-field and is denoted $\vec{H}(\vec{r})$ below.

In these simulations, the current flow in the sample is two-dimensional. The sample is a thin rectangle of thickness t with the normal along z . The currents are independent upon z and flow along x and y only. In this case one may write:¹⁶

$$\vec{j}(\vec{s}) \equiv \nabla_{\vec{s}} \times [g(\vec{s}) \hat{z}] \quad (1)$$

substitution in the Biot and Savart formula¹⁷

$$\vec{H}(\vec{r}) = \frac{1}{4\pi} \int_V \vec{j}(\vec{s}) \times \frac{\vec{r} - \vec{s}}{|\vec{r} - \vec{s}|^3} d^3s \quad (2)$$

yields after some calculations¹⁸ and spatial discretization to pixels of size a^2 the following equation for the component of the self-field along z in a plane parallel to the sample and at a distance d from the sample:

$$H_z(i, j, d) = \frac{1}{4\pi} \sum_{k,l} g(k, l) \int_{k-1/2}^{k+1/2} \int_{l-1/2}^{l+1/2} \int_0^t \frac{2(d+\zeta)^2 - a^2(\xi-i)^2 - a^2(\eta-j)^2}{[(d+\zeta)^2 + a^2(\xi-i)^2 + a^2(\eta-j)^2]^{5/2}} d\zeta d\eta d\xi, \quad (3)$$

where ξ , η , and ζ are along x , y , and z , respectively. The (integer) pixel coordinates in the sample are (k, l) and in the plane where the H_z field is calculated these coordinates are (i, j) . This equation can be written as

$$H_z(i, j, d) = \frac{1}{4\pi} \sum_{k,l} M(i, j, k, l) g(k, l), \quad (4)$$

where $M(i, j, k, l)$ is the integral shown in Eq. (3). Although not explicitly written, $M(i, j, k, l)$ depends on the sample thickness t and the distance d between the plane of observation and the sample surface. For the simulations it is assumed that the current density is uniform throughout the sample.¹⁹ From Eq. (1) follows that g can then be constructed as the height of a hip roof with fixed slope (i.e., the current density) and the sample circumference as base. The matrix $M(i, j, k, l)$ is calculated from the geometry of the sample

and the plane of observation. The self-field is then found from matrix multiplication as defined by Eq. (4).

To model a twin plane, we define a line in the sample (connected to its edge) and take the current across the line to be zero; this is equivalent to considering the twin plane as an extension of the edge of the sample. Using Eq. (4) and the known geometry of the sample, the self-field H_z can be numerically calculated. To compare with the shielding properties of a sample in an external field, a position independent external field is added to H_z such that for the centre of the sample $H_z = 0$. Results are presented in Fig. 1 where the current pattern is given in the left-hand panels and the calculated total H_z field in the right-hand panels.

For a rectangular sample without twin planes and with dimensions $100 \times 70 \times 1$ (arbitrary units), the result is shown in Fig. 1(a). The edge of the sample is indicated by a black line (RH panel). The familiar cushion-shaped flux penetration is found, which is also known experimentally.²⁰ In the

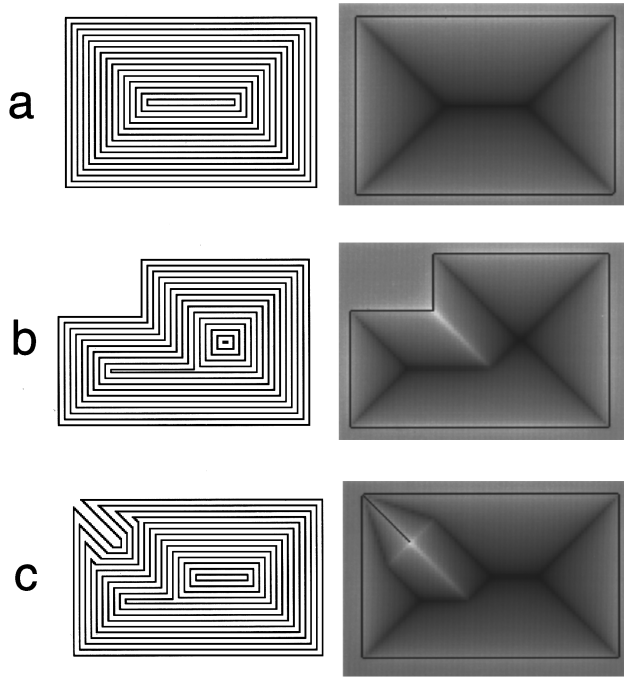


FIG. 1. Simulation of the z component of the local magnetic field H_z (right-hand panels) produced by an external field and a constant shielding current in thin samples of three different shapes. The corresponding current flow pattern is given on the left-hand panels. In (a) a rectangular sample yields the familiar cushion shaped pattern, while in (b) the effect of an inward pointing corner is shown. In (c) a sample with a line defect in the upper left hand corner is shown. No current flows across this defect. At the end of this defect, the local field is 45% above the external field.

middle of the edges of the sample the local field is higher than the applied field by about 20%. This is easily understood because the shielding current generates a field opposite in sign to the applied field in the inside of the sample, but parallel to the applied field outside the sample: close to the edge of the sample the shielding current enhances the external field.

In Fig. 1(b) the effect of an inward pointing corner (top left) is shown. Clearly a high local field inside the sample arises due to this corner, which will cause enhanced flux penetration. Hence any damage to the edge of a thin sample may significantly influence the flux penetration.

In Fig. 1(c) the effect of a short twin plane in the upper left corner is shown. The twin is indicated by a black line. As stated above, the twin may be considered as an edge of the sample. The shielding currents which flow around the twin enhance the local field in the twin because the shielding currents enhance the local field outside the sample and thus also in the twin. This effect is so strong that for the geometry shown the local field at the end of the twin is 45% higher than the external field. Since flux penetration is driven by the nucleation of vortices at the edge of the sample, such a strong local field will enhance the injection of vortices at the end of the twin. Of course in the real sample the current across the twin is only reduced and not zero. Nevertheless the same argument still holds: at such a defect the flux penetration is enhanced.

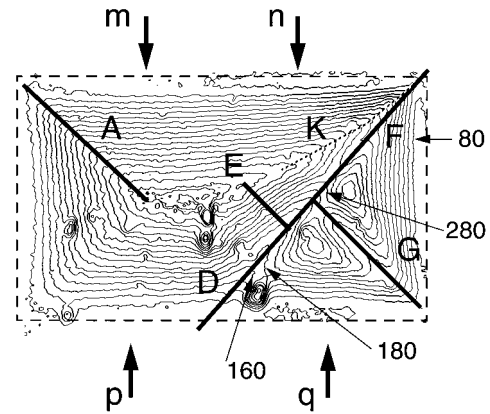


FIG. 2. The flux front (see text for definition) in a $\text{YBa}_2\text{Cu}_3\text{O}_7$ sample with two twin planes (DF and G) for several values of the external field as indicated (values are in mT). The dashed line shows schematically the edge of the sample, while the thin wiggly lines are the fluxfronts. The flux penetration at (n) is hindered with respect to penetration at (m), due to the presence of the twin plane DF . The other lines and labels are explained in the text.

IV. FLUX FLOW ALONG AND ACROSS TWIN PLANES

To study the penetration of flux in a virgin sample, the $\text{YBa}_2\text{Cu}_3\text{O}_7$ single crystal was cooled in zero field to 2 K. Subsequently, the field was increased at a rate of 20 mT/s. As soon as the external field exceeds a certain value, flux starts to penetrate the sample. The density of this flux is highest at the edges of the sample and decreases towards its interior. The flux front is defined as the edge of the region where the flux density is still zero. For practical purposes, in particular to reduce the noise in the analysis, we have chosen a flux density slightly above zero as the experimental flux front. In Fig. 2 the experimental flux fronts are depicted as a function of external field. Each wiggly line corresponds to a flux front at a certain applied field. Between two consecutive flux front lines, the external field was increased by 20 mT; for some flux fronts the corresponding field in mT is indicated in the figure. The edge of the sample is schematically indicated by dashed lines, the twin planes are at the thick lines marked (D), (F), and (G). Some defects in the EuSe film show up as small circular areas with a high density of flux front lines.

To discuss the flux penetration we define a flux penetration rate dx/dH_{ext} where x is the distance the flux front has penetrated from the edge and H_{ext} is the applied external field. At low fields (e.g., 100 mT) the flux penetrates very slightly and the flux front is most advanced in the middle of the sides of the rectangular sample; the twin planes have no influence. Penetration in the middle of the sides in a rectangular sample is normally observed in defect-free samples²⁰ and is due to the fact that the self-field of the sample enhances the externally applied field most in the middle of the edges of the sample, see also Fig. 1(a). In the experiment at fields above 100 mT, the flux penetration rate dx/dH_{ext} is large along the twin planes as can be seen from the large distance between the flux front lines along the twin planes (D), (F), and (G). To show in detail the effect of the twin planes on the flux penetration we have plotted in Fig. 3 the

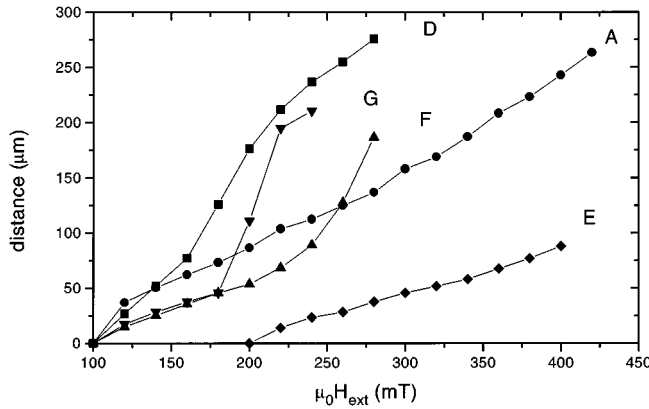


FIG. 3. Distance of the fluxfront from the 100 mT fluxfront as a function of external field and along the lines indicated in Fig. 2. Penetration along the twinplanes D , F , and G is at a certain stage faster than elsewhere. Penetration sideways from the twins, e.g., along E is approximately the same as in untwinned regions (see text).

position of the flux front as a function of external field along the lines marked (A), (D), (E), (F), and (G) in Fig. 2. At line (A), there is no twin plane and the flux front progresses linearly as a function of applied field: dx/dH_{ext} is not dependent upon H_{ext} . By contrast, there is a twin plane present at the geometrically equivalent line (G). Along this line, at first the flux penetrates in about the same way as along line (A), but above 180 mT the flux penetration rate is much higher until the flux front meets the flux penetrating along the twin plane (D) at 220 mT. Something similar happens for the flux penetrating along lines (D) and (F); above 160 mT for (D) and 240 mT for (F) the flux penetration speed is high until the fronts moving along (D) and (F) meet. The differences in flux penetration along the twin planes, in particular (F) and (G) probably reflects relative differences in impurity and atomic disorder among the twin boundaries. The flux front which penetrates perpendicular from the twin plane along the line (E), moves in at about 75% of the flux penetration rate in the middle of the sides. From the geometry the side penetration rate is expected to be about $\sqrt{2}$ lower than that from the corner along line (A); in fact the slope of line (A) divided by the slope of line (E) is ~ 1.75 . The fact that the penetration along a twin is initially as slow as elsewhere, but then shoots upwards, might be due to an inherent instability in the flux penetration process. As explained in Sec. II, current flowing around an inward pointing corner or a twin generates a high local field inside the sample. A scenario would thus be possible where at first the current flows along the edge of the sample, with a slight deviation at the position of the defect due to reduced pinning, which deviation causes locally a slightly higher field. While the external field increases, so does the shielding current, thereby enhancing the local field in the sample at the defect. Due to this, extra flux starts to penetrate, and the current has to deviate further, leading to even stronger fields and faster penetration. This process enhances the flux penetration in the twin plane which is already higher than elsewhere due to reduced pinning and only stops when the flux fronts meet and the penetrating flux is repelled by the flux already present.

Repulsion of flux penetrating outside the twin by the flux already present in the twin is clearly seen in Fig. 2 by comparing the flux penetration at the twin free region (m) with the region close to the twins (n). Close to the twins the flux fronts are closer together: the flux penetrates slower there. This behavior is probably due to the current loop around the twin, which generates a large local field with the same sign as the penetrating flux. This large local field then repels the vortices moving in the sample and hampers the flux penetration close to it.

Another effect of the twin planes is a change in the so-called discontinuity lines. These are lines where the current density is reduced due to a change in direction of the current flow; also flux penetration is normally reduced along these lines. In isotropic rectangular samples they are normally at 45° with respect to the sample edges: for example, line (A) is a discontinuity line, and also one would be expected at (F). Due to the presence of the twin plane at (F), however, this discontinuity line is split into two, one just below (F) (not indicated) and one above (F) at (K), indicated by a dotted line.

Flux penetration along twin planes was previously reported at 56 K and in fields below 50 mT by Duran *et al.*,⁵ although their earlier results were less clearcut than the present data. Later, Vlasko-Vlasov *et al.*⁶ observed that at 63 K in fields of order 10 mT flux is concentrated in front of the twin boundaries and diluted behind them, suggesting that the twin planes act as barriers which guide the motion of vortices which penetrated elsewhere just “as drifting snow is guided by a fence.” In the present experiment at 2 K we monitor the progression of the flux front as it enters the sample and do not observe guided motion but rather find that the flux penetrates along the twin planes, as found previously at higher temperatures by Welp *et al.*⁷ The flux front is most advanced along the twin planes, even in the twins that start at the corners of the sample, where in the absence of twins the flux penetration would have been less than elsewhere. Furthermore, if guiding would be dominant, then the flux should pile up in front of the twin at (q), while it would be able to move in freely at (p). As a consequence the flux density close to the twin plane should be higher at (q) than at (p), leading to a flux front which is asymmetric with respect to the twin plane. In our experiment at 2 K a practically symmetric flux front is observed around line D , i.e., the flux penetrates the sample laterally from the twin planes as if the twin planes were part of the edge of the sample. However, it should be noted that close to the flux front the flux density in the twin is of course lower than at the edge of the sample.

The presence or absence of barrier effects may depend significantly on sample properties such as the angle of the twin boundary with the natural flux gradient and the relative strength of pinning in the boundary and in the bulk. In particular, Groth *et al.*¹² have shown that the angle at which the barrier effect changes to a channel effect varies systematically with the relative pinning strength of the bulk and boundary. In our measurement at low temperature and fields up to 0.5 T the flux penetrates in the twin planes and “guiding” of flux external to the twin planes (like “drifting snow along a fence”) is not observed on flux entry. This “guidance on entry” should be distinguished from another type of guidance that occurs under the action of a driving Lorentz

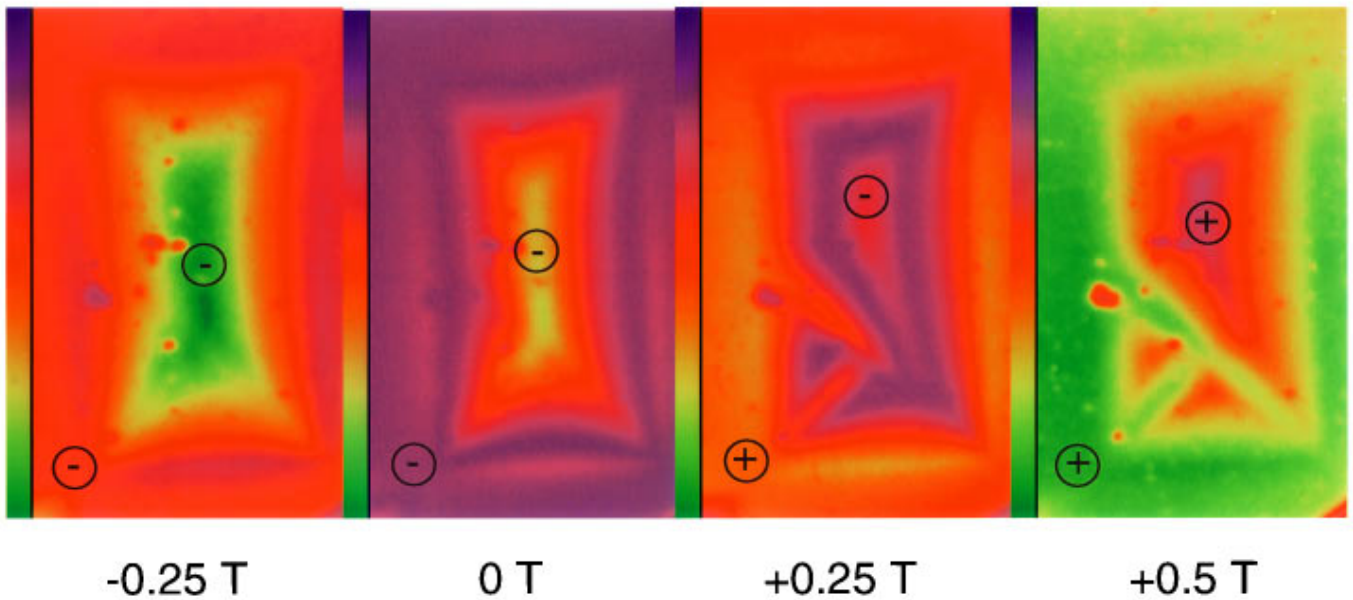


FIG. 4. (Color) Four magneto-optical images taken during a full hysteresis loop. Dark areas are represented as blue and bright areas as green (see bar). The loop is traversed between -1 and $+1$ T, and from the left towards the right picture. Flux is shown to penetrate easily along the twin planes, but for flux leaving the sample the twins seem to be not relevant. Some cosmetic defects in the EuSe layer show up as dots.

force after full penetration, which has been observed in numerical simulations.²¹

V. ASYMMETRY BETWEEN FLUX ENTERING AND LEAVING THE SAMPLE

In the previous section it was shown that the flux enters the sample preferentially along twin planes when the external field is increased. In fact this was known previously and has been reported by many authors mentioned in the Introduction. For flux leaving the sample in decreasing external field Welp *et al.*⁷ also observed that flux leaves the sample preferentially along the twins at 40 K. By contrast in our experiment at low temperature (2 K) it is surprisingly found that there is practically no influence of twin planes on flux leaving the sample when the external field is decreased, as will be shown now.

In Fig. 4 we show a few images taken during a hysteresis loop between -1 T and $+1$ T while the field was swept at 10 mT/s. The external field for each image is indicated. Before the recording of these images, the sample was zero field cooled and then cycled between $+1$ T and -1 T. They were taken in the following order: -0.25 T, 0 T, $+0.25$ T, and $+0.5$ T. It is important to note that these intensity images do not show the sign of the field, therefore the sign is indicated by \pm signs. Just after passing through zero external field, in the image at $+0.25$ T, deep penetration of flux along the twin planes is observed, similar to the penetration discussed above for the zero field cooled sample. Remarkably, when the field is decreased, as shown in the images for -0.25 T, and 0 T, the flux does not leak out along the twin planes at (F) and (G), and only slightly along the twin plane at (D) (barely visible in the figure). It must be stressed here that one should be careful with the interpretation of magneto-optical intensity images close to zero field since the intensity is qua-

dratically dependent on the local field, and not linearly. For this reason we show in Fig. 5 contour lines of the local field and not the intensity. Figure 5(a) is for $+0.25$ T, while Fig. 5(b) is for 0 T. Although a slight effect of the twin on the flux leaving the sample is visible at (TP) in Fig. 5(b), it is evident that indeed the effect of the twins is very small when

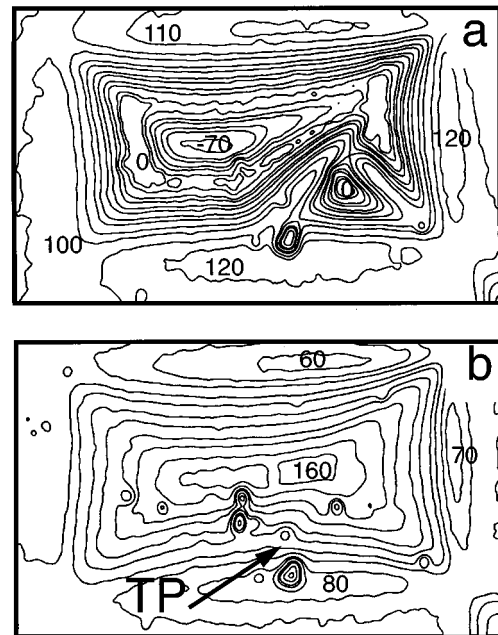


FIG. 5. Contours of the local magnetic field component H_z , expressed in mT for two images of Fig. 4: (a) is at $+0.25$ T and (b) is at 0 T external field. Although at (TP) some effect of the twin can be seen, there is very little influence of the twin on flux leaving the sample, while the effect on the penetrating flux as seen in (a) is very important.

the flux is leaving the sample. Now the possible origin for this asymmetry will be discussed.

Since the width of the twin plane is much smaller than the superconducting penetration depth λ , vortices in the twin plane can in principle be pinned by other vortices adjacent to the twin. Then the vortices in the twin would be completely locked in the vortex lattice of the bulk material. This situation occurs when the sample is full of flux, e.g., at -0.25 T or at 0 T in Fig. 4, in this case the vortices in the twin are completely locked by the surrounding vortices (which themselves are strongly pinned in the bulk at these temperatures) and thus cannot move along the twin. By contrast, when flux enters a zero field cooled sample it can flow easily along the twin planes because in this case there is no such locking possible, since there are no vortices close to the twins yet. Similarly vortices which penetrate the sample after increasing the external field from -1 T to values above 0 T, are of opposite sign compared to those already present in the bulk. In this situation the penetrating vortices are attracted towards the bulk, where they can annihilate with their antivortices: also in this situation no locking occurs.

To sum up, at low temperature flux may enter easily along twin planes, but if flux is present throughout the sample, it will not preferentially leave along the twin planes. As a consequence, depending on the flux pattern present in the sample, the twins may have or not have an influence on the critical current j_c and on the current flow pattern in the sample. The difference between this low temperature behavior and that observed at 40 K by Welp *et al.*⁷ should be investigated further, e.g., by the model of Groth *et al.*¹² and may depend on the ratio between twin boundary pinning and bulk pinning.

VI. INFLUENCE OF TWIN PLANES ON CURRENT FLOW

In this section we derive from magneto-optical measurements the local current flowing in the sample. For this purpose we use a recently developed scheme,¹⁸ which is based upon numerical inversion of Eq. (4).

First the cosmetic defects are removed from the magneto-optical images, then the local field $H_z(i,j)$ as a function of position in the magneto-optical film above the sample is calculated as discussed in Sec. II. Using the known thickness of the sample and the known distance between sample and magneto-optical layer, the geometrical matrix $M(i,j,k,l)$ is calculated. In fact, if the distance is much smaller than the thickness, $M(i,j,k,l)$ becomes independent upon distance. Typically a measured $H_z(i,j)$ image is a 500×700 matrix and $M(i,j,k,l)$ contains $\sim 10^{11}$ elements, which makes the inversion nontrivial. However, due to the symmetry properties of $M(i,j,k,l)$, which is a Toeplitz block Toeplitz matrix, efficient storage is possible. The inversion is carried out on an IBM SP2/9076 machine using 16 parallel processors.

The inversion of Eq. (4) yields $g(k,l)$ and the current as a function of position (k,l) in the sample is obtained through Eq. (1). Since the present sample is very thin, the assumption of 2D current flow is reasonable. We stress that also the flow pattern of the current is a result of the calculation. Contrary to the simulation presented in Sec. II, for the analysis of the experimental results there is no assumption made *a priori* as to the shape of the current flow pattern; it is not even im-

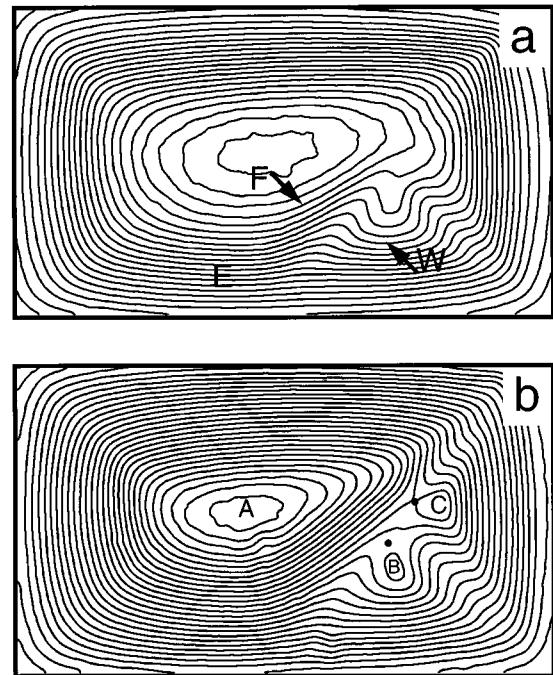


FIG. 6. Flow lines of the current for (a) 0.24 T and (b) 0.81 T external field. A larger distance between the flow lines indicates a lower current density. The current density in the front of the twin at (F) is the same as along the edge at (E), but higher than in the wake of the twin at (W). At 0.81 T very clearly subloops of the current flow are formed around (A), (B), and (C). Nodal points with zero current density are indicated by the dots above (B) and left of (C).

posed that the current should flow in the sample only.

In Fig. 6(a) the flow lines of the current [which are the contour lines of $g(k,l)$] are shown at an applied field of 0.24 T after zero field cooling. At the twins the flow lines are further apart than next to the twins: the current density in the twins is about half of the current density elsewhere. This is consistent with the magnetization measurement of Oussena *et al.*⁴ In the wake (W) of the long twin, the current density is lower than in front (F) of it: the twin deflects the current flow. Indeed some of the current is flowing only left of the long twin, i.e., part of the current shields only the left half of the sample. The current density in front (F) of the long twin is not higher than along the edge of the sample, e.g., at (E). At the scale of detail resolved in the present experiment no enhanced j_c is observed in front of the twin plane, although such enhancement in a very narrow region close to the twin as shown sometimes in schematic pictures^{13,6} cannot be ruled out. If the field is increased further, e.g., to 0.81 T, more subloops of the current are formed, see Fig. 6(b). Most of the current circulates left of the twins around (A), but there are two other current loops: around (B) and (C), notwithstanding that part of the current still flows around the whole sample. We note that if in the analysis of bulk magnetization measurements all the current is assumed to flow around the whole sample (instead of taking the subloops into account) too low j_c values will be calculated.

The effect of the twins on the current flow is shown in a more vivid way in Fig. 7, which is a different representation of the measurement already shown in Fig. 6(a) at 0.24 T. In

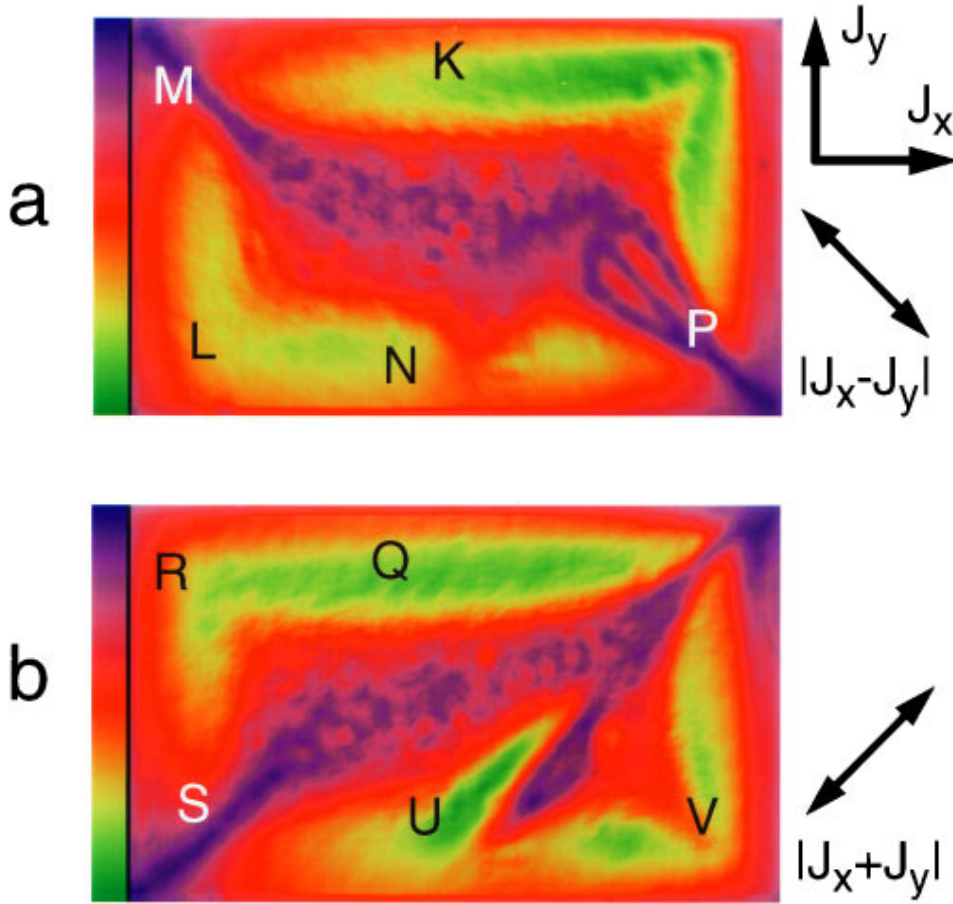


FIG. 7. (Color) Component of the current density vector along (a) NW-SE and (b) SW-NE, as indicated by the arrows, for the current flow shown in Fig. 6(a) at 0.24 T. The current is flowing around the twin at (P) and (U), while the current across the twins is reduced by about 50% as seen at (N) and (V). The other labels are explained in the text.

this figure the absolute value of the current density is shown as a color value, which is blue for zero current and green for the highest currents. Figure 7(a) shows the absolute value of the component of the current density vector which is flowing in the NW-SE direction as indicated by the arrow, while Fig. 7(b) shows the component along SW-NE. The current density at the edge in (L) is the same as along the sides of the sample [e.g., at (K)], as is seen from the same color values in the picture. This is because at (L) in Fig. 7(a) all the current is flowing NW-SE while the current density is reduced by a factor $\sqrt{2}$ because of the 90° angle in the current flow direction, whereas at (K) all the current flows parallel to the side of the sample and its component along NW-SE is a factor $\sqrt{2}$ lower. Of course, at (M) all the current flows NE-SW and hence the component along NW-SE is zero. Similarly in Fig. 7(b) the component of the current along NE-SW is the same at (R) and (Q), while it is zero at (S). More interesting is the behavior at the twin planes. In Fig. 7(a) the component of the current is shown which crosses the twin plane at (N) at 90° . The current density across the twin plane is found to be about half of the value elsewhere, while the component along the twin plane is significantly enhanced as shown at (U). In fact most of the current flows only along the twin at the left-hand side, because it is part of a subloop like the one shown in Fig. 6(b) at (A). In the twin plane at (V) again a reduction to about half of the current is observed [compare (V) with (R)], while one can see clearly at (P) that the current flows along this twin [compare (P) with (M)].

The above observation, i.e., low current density across twins and easy flux penetration along twins are at first sight at variance with the reported higher critical current in heavily twinned crystals. In particular Dorosinskii *et al.*^{13,14} report strong pinning in heavily twinned regions. First of all it should be stressed that those measurements indicate strong pinning at temperatures around 60 K, while our experiment is at 2 K, where the pinning behavior may be different. A strong temperature dependence of the influence of twin planes on resistance,¹ pinning² and magnetization^{3,4,22} was found previously. Second, we find at low temperature that in a fully penetrated sample there is no easy movement along the twins any more, while the twins most probably do lead to extra pinning because of the different superconducting properties of the twins.⁶ Upon first penetration after zero field cool, the flux enters quickly along the twins, but after this initial stage further flux penetration is hindered by the flux in the twin planes and then also increased effective pinning is expected.

To sum up, the current density for current flowing across twins is reduced for the case where flux enters along the twins (increase of field after zero field), while it is essentially unaffected in the twins if the field is decreased.

VII. CONCLUSIONS

We have investigated the behavior of isolated twin planes in $\text{YBa}_2\text{Cu}_3\text{O}_7$ at low temperature and high magnetic field. By comparing the flux fronts as a function of external field in

front of and in the wake of a twin plane, we conclude that flux penetrates in the twin plane and is not guided along it ('like drifting snow is guided along a fence'). Flux present in a twin plane reduces flux penetration in regions of the sample close to the twin. Flux penetrates easily along the twin planes, but for flux leaving the sample the twin planes have much less influence.

We determined the local current density vector using the magneto-optical technique in combination with a new calculational scheme. The current density across a twin plane is about half of its value elsewhere. Depending on the applied external field, current subloops may form in the sample.

The higher average critical currents in twinned crystals as a whole as compared to detwinned ones is explained by a combination of several effects: (i) in a fully penetrated sample there is no easy movement along the twins any more, (ii) the twins most probably do lead to pinning due to the different superconducting properties of the twins, (iii) flux movement across twins is always hindered, and (iv) although upon first penetration after zero field cool, the flux enters

easily along the twins, after this initial stage further flux penetration is hindered by the flux in the twin planes and increased effective pinning is expected.

ACKNOWLEDGMENTS

We thank J. C. Martinez for drawing our attention to the interesting properties of the present sample, N. C. Svanberg for aid with the measurements, H. J. W. Spoelder for aid with the software implementation of Eq. (4) and G. W. Crabtree, U. Welp, M. V. Indenbom, and R. Surdeanu for useful discussions. This work was part of the research program of the Stichting Fundamenteel Onderzoek der Materie (FOM), which is financially supported by the Nederlandse Organisatie voor Wetenschappelijk Onderzoek (NWO). This work was supported by the U. S. Department of Energy under Contract No. W-31-109-ENG (W.K.K.) and by the U. S. National Science Foundation Science and Technology Center for Superconductivity under Contract No. DMR 91-20000 (J.F.).

-
- ¹W.K. Kwok, U. Welp, G.W. Crabtree, K.G. Vandervoort, R. Hulscher, and J.Z. Liu, *Phys. Rev. Lett.* **64**, 966 (1990).
- ²E.M. Gyorgy, R.B. van Dover, L.F. Schneemeyer, A.E. White, H.M. O'Bryan, R.J. Felder, J.V. Waszczak and W.W. Rhodes, *Appl. Phys. Lett.* **56**, 2465 (1990).
- ³M. Oussena, P.A.J. de Groot, S.J. Porter, R. Gagnon, and L. Taillefer, *Phys. Rev. B* **51**, 1389 (1995).
- ⁴M. Oussena, P.A.J. de Groot, K. Deligiannis, A.V. Volkosub, R. Gagnon, and L. Taillefer, *Phys. Rev. Lett.* **76** 2559 (1996).
- ⁵C.A. Duran, P.L. Gammel, R. Wolfe, V.J. Fratello, D.J. Bishop, J.P. Rice, and D.M. Ginsberg, *Nature* **357**, 474 (1992).
- ⁶V.K. Vlasko-Vlasov, L.A. Dorosinskii, A.A. Polyanskii, V.I. Nikitenko, U. Welp, B.W. Veal, and G.W. Crabtree, *Phys. Rev. Lett.* **72**, 3246 (1994).
- ⁷U. Welp, T. Gardiner, D. Gunter, J. Fendrich, G.W. Crabtree, V.K. Vlasko-Vlasov, and V.I. Nikitenko, *Physica C* **235-240**, 241 (1994).
- ⁸M. Turchinskaya, D.L. Kaiser, F.W. Gayle, A.J. Shapiro, A. Roytburd, V. Vlasko-Vlasov, A. Polyanskii, and V. Nikitenko, *Physica C* **216**, 205 (1993).
- ⁹H. Safar, S. Foltyn, H. Kung, M.P. Maley, J.O. Willis, P. Arendt, and X.D. Wu, *Appl. Phys. Lett.* **68**, 1853 (1996).
- ¹⁰C.A. Duran, P.L. Gammel, D.J. Bishop, J.P. Rice, and D.M. Ginsberg, *Phys. Rev. Lett.* **74**, 3712 (1995).
- ¹¹U. Welp, T. Gardiner, D.O. Gunter, B.W. Veal, G.W. Crabtree, V.K. Vlasko-Vlasov, and V.I. Nikitenko, *Phys. Rev. Lett.* **74**, 3713 (1995).
- ¹²J. Groth, C. Reichhardt, C.J. Olson, S. Field, and F. Nori, *Phys. Rev. Lett.* **77**, 3625 (1996).
- ¹³L.A. Dorosinskii, M.V. Indenbom, V.I. Nikitenko, A.A. Polyanskii, R.L. Prozorov, and V.K. Vlasko-Vlasov, *Physica C* **206**, 360 (1993).
- ¹⁴L.A. Dorosinskii, V.I. Nikitenko, A.A. Polyanskii, and V.K. Vlasko-Vlasov, *Physica C* **219**, 81 (1994).
- ¹⁵R.J. Wijngaarden *et al.* (unpublished).
- ¹⁶E.H. Brandt, *Phys. Rev. B* **46**, 8628 (1992).
- ¹⁷J.D. Jackson, *Classical Electrodynamics*, 2nd ed. (Wiley, New York, 1975), Eq. (5.14).
- ¹⁸R.J. Wijngaarden, H.J.W. Spoelder, R. Surdeanu, and R. Griesen, *Phys. Rev. B* **54**, 6742 (1996).
- ¹⁹In real samples the current flowlines become curved at the inward pointing defects leading to deviations from uniform flow. However, the arguments that follow are qualitatively unaffected. For a further discussion see Th. Schuster, H. Kuhn, and E.H. Brandt, *Phys. Rev. B* **54**, 3514 (1996).
- ²⁰M.R. Koblishka and R.J. Wijngaarden, *Supercond. Sci. Technol.* **8**, 199 (1995).
- ²¹G.W. Crabtree, G.K. Leaf, V.M. Vinokur, A.E. Koshelev, D.W. Braun, D.M. Levine, W.K. Kwok, and J.A. Fendrich, *Physica C* **263**, 401 (1996).
- ²²U. Welp, W.K. Kwok, G.W. Crabtree, K.G. Vandervoort, and J.Z. Liu, *Appl. Phys. Lett.* **57**, 84 (1990).